Magnetic Field-Line Reconnection in a Toroidal Plasma

S. Iizuka, Y. Minamitani, and H. Tanaca
Research Institute for Energy Materials, Yokohama National University, Yokohama 240, Japan

and

Y. Kiwamoto
Plasma Research Center, University of Tsukuba, Ibaraki 305, Japan
(Received 9 February 1984)

The magnetic field-line reconnection is investigated in detail by rapidly reversing the toroidal current in a torus plasma. The reconnection brings about an explosive increase in the plasma pressure in a quite narrow region where a shocklike structure is observed. A strong plasma acceleration and an anomalous resistivity due to the reconnection are estimated by the magnetohydrodynamics equations with the variables obtained from the experiment.

PACS numbers: 52.35.Mw, 52.25.Fi, 52.30.+r

Magnetic field-line reconnection[1] in a plasma causes efficient plasma heating and plasma acceleration in a narrow region.[2] It is believed that solar flares and magnetospheric substorms are closely related to the reconnection.[3] Experiments on the reconnection have been performed in finite-size laboratory plasmas,[4,5] where the plasma boundary and electric field due to space charges[6] might affect the evolution of the reconnection. Kadomtsev[7] predicted that the reconnection should appear in the internal disruption of tokamak plasma, among the auxiliary field B_p^* in place of the actual poloidal magnetic field B_p. Kadomtsev's model was examined with computer simulation,[8] although in experiment the closest observation has been performed via soft x-ray measurement.[9] Here we report direct observation of reconnections among poloidal field lines in a current-carrying toroidal plasma.[10] In the toroidal direction this experiment is free from space-charge effects associated with electrodes, and simulates well Kadomtsev's model in terms of the observable field B_p.

The experiment is carried out in a small tokamak[11] (major radius $R = 12$ cm, minor radius $a = 3$ cm) made of a Pyrex glass surrounded by a copper shell with slits in the toroidal and poloidal directions through which the electric field can penetrate as shown by Fig. 1(a). Loop voltage is ~ 20 V and toroidal current is 0.5–1 kA. Argon gas of $\sim 1.45\times10^{-2}$ Pa is discharged in the toroidal magnetic field (~ 3 kG) by the electric field induced by the pulsed primary current. The reverse field is triggered at 100–120 μs after the start of the discharge (duration of ~ 150 μs), where the toroidal current and plasma density gradually decrease from the maxima. That is, after having performed the usual Joule heating and established the initial B_p distribution over the plasma cross section, the polarity of the induced electric field is reversed ($t = 0$), then the total toroidal current quickly changes polarity in a few microseconds. Following the current reversal the region of reversed B_p field starts forming on the plasma surface first and then penetrates into the core pushing out the region of the initial B_p distribution. It is between the two regions that the reconnection proceeds drastically. All components of the magnetic field B_p are measured by a 1-mm-diam, 10-turn-loop magnetic probe. The electron density n_e and temperature T_e are measured by a 2.5-mm-long double probe. The probe current is measured at a constant voltage which is changed every five shots for statistical average. We employ the cylindrical coordinate sys-

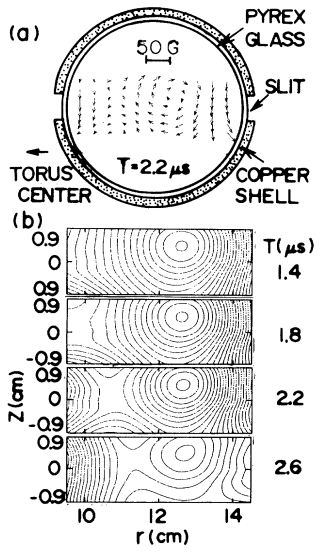

FIG. 1. (a) Cross section of a torus with the poloidal magnetic-field configuration $\vec{B}_p$ at $t = 2.2$ μs; (b) Contour plots of the magnetic flux function ψ_1 in arbitrary units with time t as a parameter.

tem of r (major radius), θ (toroidal direction), and z (major axis). The two-dimensional evolution of the plasma parameters in the cross section is measured at 11×7 $(r\times z)$ mesh points inside the rectangular region of $|z|\leq 0.9$ cm and 9.5 cm $\leq r \leq 14.5$ cm. All data are recorded in a memory disk and processed by a computer.

Figure 1(a) shows a typical field B_p in the cross section. To confirm the reconnection we calculate the magnetic flux function ψ from measured values of $\vec{B}_p=(B_r,B_z)$,

$$\psi=\psi_0+\psi_1,\quad \psi_1=\int_R^r rB_z\,dr-\int_0^z rB_r\,dz. \tag{1}$$

Here, the flux $\psi_0=\int_0^R rB_z\,dr$ is a time-dependent constant which does not affect the profile of ψ. Thus, we plot only the contour of ψ_1 in Fig. 1(b) to show the topological change of the magnetic field lines through the reconnection. Although ψ_1 distributes almost circularly for $t\lesssim 1.2$ μs, its shape is strongly modified for $t\gtrsim 1.2$ μs and an x-type separatrix is formed inside the torus ($r\simeq 9.5$ cm). There the magnetic field lines of the reversed and forward directions are reconnected and the magnetic neutral point comes out, that is, a reconnection region (RR) appears. Since the forward B_p lines are forced to disappear by the reconnection, the reversed-current layer can penetrate inside the plasma faster than the skin time. The initial B_p region diminishes with time and eventually vanishes for $t\gtrsim 3$ μs, and the circular ψ_1 associated with the reversed current occupies the whole region.

The spatial profile of the current density J_θ at $z=0$, calculated from

$$J_\theta=(\partial B_r/\partial z-\partial B_z/\partial r)/\mu_0, \tag{2}$$

is plotted in Fig. 2(a). The current J_θ has a maximum at $r\simeq 12.5$ cm for $t<0$, in agreement with the position of the magnetic axis in Fig. 1. The current J_θ starts decreasing at $t=0$ and changes polarity near the periphery first. The region of reversed current penetrates inward faster than the magnetic diffusion time ($\tau_D\simeq 110$ μs) determined by the classical resistivity η_c derived from the average initial electron temperature $T_e\simeq 17$ eV. The penetration velocity is slow in the beginning, but after ~ 1.2 μs it increases to $\sim 2.2\times10^5$ cm/s, being about 3×10^{-2} times as large as the Alfvén velocity $v_A\simeq 7.3\times10^7$ cm/s calculated from the total magnetic field (~ 3 kG) and $n_e\simeq 2\times10^{12}$ cm^{-3} at $t=0$. The reversed current has a peak around the RR and such a peak also moves with the RR as shown by the arrow.

Simultaneously, a remarkable deformation of the plasma-pressure distribution is observed in Fig. 2(a). Before the current reversal, the pressure $P\simeq n_eT_e$ distributes almost the same as J_θ. At $t=0$, P at $r\lesssim 10$ cm starts increasing rapidly and the spatial profile of P peaks in the RR. We note here that the peak of P moves with the RR only in the initial stage of the reconnection ($t\lesssim 2.5$ μs), but later it gradually gets behind the RR as indicated by the arrow. Such a lag might be attributed to the quick plasma outflow from the RR as a result of the strong pressure gradient.[12] The evolution of P at the inner periphery $A(r,z)=A$(10 cm, 0 cm) and the center B(12 cm, 0 cm) are shown in Fig. 2(b). The total toroidal current I_θ is also plotted by the dotted curve. At A where the RR passes, after quickly rising to the maximum at $t\simeq 1.8$ μs, P and n_e drop rapidly in spite of the continuous current increase. The time to reach the maximum of P and n_e coincides well with the time at which the RR passes A as indicated by the arrow. Thus the plasma heating and particle accumulation effectively take place in the RR, not simply as a result of the joule heating due to J_θ. On the contrary, P and n_e at B decrease during the reconnection, indicating particle loss through the RR. At the position (14

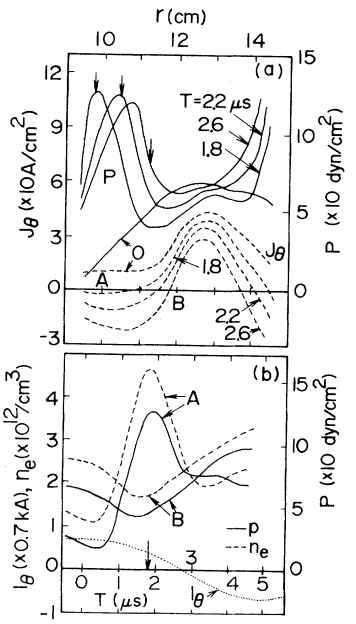

FIG. 2. Radial profiles of (a) toroidal current density J_θ (broken curve) and pressure P (solid curve) with time t as a parameter. The arrow shows the position of the reconnection region. (b) Temporal evolution of the pressure P (solid curve) and density n_e (broken curve) at positions A and B shown in (a). The dotted curve shows variation of total toroidal current I_θ. The reconnection layer passes A at $t=1.8$ μs as indicated by arrow.

cm, 0 cm) where no reconnection occurs, we did not observe a clear peaking of P and n_e except a slow increase due to the joule heating by J_θ.

The two-dimensional plots of J_θ and P at $t=2.2$ μs are shown in Figs. 3(a) and 3(b), respectively. Comparing with Fig. 1, we find that the strong J_θ and P regions almost coincide with but lag slightly behind the position of the RR. In order to estimate the transport the plasma flow $\vec{v}=(v_r, v_z)$ is calculated from the magnetohydrodynamic equations of motion and continuity,

$$\rho_m d\vec{v}/dt = \vec{J}_\theta \times \vec{B}_p - \vec{\nabla} P, \quad d\rho_m/dt = 1, \qquad (3)$$

where $d/dt = \partial/\partial t + v\cdot\vec{\nabla}$, ρ_m ($\simeq n_e m_i$) is the mass density, m_i the ion mass, q the effective ionization rate including recombination. First, we distribute 4000 plasma elements of zero initial velocity in the cross section at $t=-1$ μs so as to be proportional to the actual density profile. The orbits of all elements are calculated from Eq. (3) and $d\vec{r}/dt=\vec{v}$, using the values obtained from the experiment. Although a remarkable increase in $\vec{v}$ is not obtained until $t=0$, a strong flow appears in the RR for $t>0$ as shown in Fig. 3(d). The plasma is intensely accelerated outward from the RR with the velocity of 5×10^5 cm/s. However, a dominant acceleration occurs in the z direction, especially in the RR (9.5 cm $\lesssim r \lesssim$ 10.5 cm). On the other hand, we also find a large plasma flow in the plasma center region (13 cm, 0 cm). But this flow comes out mainly as a result of $\vec{j}_\theta\times\vec{B}_p$ force pointed to the magnetic axis [see Fig. 1(b)] formed by the forward toroidal current. This effect is dominant in the center region where the pressure force is of minor contribution. Equation (3) may not hold during the reconnection when ions are weakly magnetized.[13]

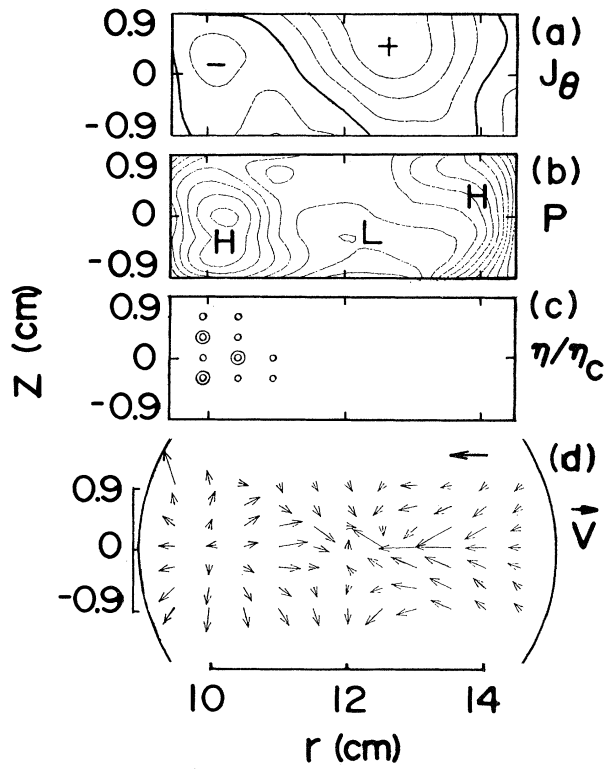

FIG. 3. Contour plots of (a) toroidal current density J_θ (contour spacing is 9.5 A/cm^2), and (b) pressure P (spacing is 12 dyn/cm^2) in the r-z plane. In (a), marks + and − correspond to the forward- and reversed-current regions, respectively, and thick curve shows the boundary $J_\theta=0$. In (b), H and L show the higher and lower P regions, respectively. (c) Resistivity normalized by the classical value, η/η_c (single open circle, 50–100; double open circle, 100–150); (d) Plasma flow vector $\vec{v}$. The upper right arrow shows the magnitude of 5×10^5 cm/s. All figures are obtained at 2.2 μs.

It was pointed out that the resistivity η plays an important role on the reconnection and energy dissipation.[2,6] We therefore evaluate η from Ohm's law in the toroidal direction:

$$\eta J_\theta = E_\theta + (v_z B_r - v_r B_z) - \frac{m_e}{e^2 n_e}\frac{\partial J_\theta}{\partial t},$$
$$E_\theta = -(\partial\psi/\partial t)/r \quad (\psi=\psi_0+\psi_1). \qquad (4)$$

Here, the above $\vec{v}$ is used. All the variables in Eq. (4) have been obtained from the experiment except for the electric field E_θ which contains ψ_0. However, if $J_\theta=0$ at $r=r_0$, the right-hand side of Ohm's law equation must vanish; then E_θ and thus $-(\partial\psi_0/\partial t)/r$ at $r=r_0$ can be determined experimentally. The spatial variation of E_θ inside the plasma can be calculated from $-(\partial\psi_1/\partial t)/r$ and Eq. (1). By averaging E_θ in the cross section the ratio η/η_c is evaluated as shown in Fig. 3(c). From the calculation we find an enhanced resistivity in the RR, while no anomaly appears in the region $r\gtrsim 14$ cm in spite of the strong reversed current there. The maximum value $\sim 7.9\times10^{-2}$ Ω cm at (10 cm, 0.3 cm) is about 1.1×10^2 times as large as η_c.

Although the reconnection does not proceed in a quasistationary state in our experiment, a shocklike structure is found in the RR around $r\simeq 10$ cm as shown in Figs. 1 and 3. A steep increase in P toward the RR and the similarly steep decrease in B_p appear simultaneously, indicating the kinetic and magnetic pressure balance in the slow shock. The decrease in P and the increase in the plasma-flow energy in the z direction around the RR also show the energy-flux conservation along the stream lines.

In conclusion, a strong pressure increase is ob-

served in the reconnection region accompanied by a localized shocklike structure, where plasma acceleration and anomalous resistivity are estimated. Using the averaged anomalous resistivity $\bar{\eta} \simeq 2.7 \times 10^{-2}$ Ω cm, the time scale and width of the reconnection are calculated from Kadomtsev's theory as $\tau = (\tau_A^* \tau_D)^{1/2} \simeq 4$ μs and $\delta = a(\tau_A^*/\tau_D)^{1/2} \simeq 3$ cm, in approximate agreement with the experiment [Fig. 1(b)]. Here, we use the poloidal Alfvén velocity v_A^* ($\simeq 7.7 \times 10^5$ cm/s) calculated from the averaged B_p as in the theory, and $\tau_A^* = a/v_A^*$ and $\tau_D = \mu_0 a^2/\bar{\eta}$.

We would like to thank Dr. Tetsuya Sato for his valuable discussions and Dr. Noriyoshi Sato for his encouragement. The work is partially supported by Grants-in-Aid for The Sakkokai and The Hattori-Hokokai Foundations (Japan).

[1]H. E. Petschek, NASA Spec. Publ. **50**, 425 (1964).

[2]T. Sato and T. Hayashi, Phys. Fluids **22**, 1189 (1979).

[3]V. M. Vasyliunas, Rev. Geophys. Space Phys. **13**, 303 (1975).

[4]A. Bratenahl and C. M. Yeates, Phys. Fluids **13**, 2696 (1970).

[5]J. Ohyabu, S. Okamura, and N. Kawashima, J. Geophys. Res. **79**, 1977 (1974).

[6]R. L. Stenzel and W. Gekelman, Phys. Rev. Lett. **42**, 1055 (1979).

[7]B. B. Kadomtsev, Fiz. Plazmy **1**, 710 (1975) [Sov. J. Plasma Phys. **1**, 389 (1975)].

[8]A. Sykes and J. A. Wesson, Phys. Rev. Lett. **37**, 140 (1976).

[9]J. D. Callen and G. L. Jahns, Phys. Rev. Lett. **38**, 491 (1977).

[10]Y. Kiwamoto, in Fusion Energy–1981, Selected Lectures Presented at a Spring College on Fusion Energy, Trieste, Italy, 1981, International Atomic Energy Agency Report No. IAEA-SMR-82 (unpublished).

[11]Y. Kiwamoto, H. Kuwahara, and H. Tanaca, J. Plasma Phys. **21**, 475 (1979).

[12]T. Sato, private communication.

[13]W. Gekelman, R. L. Stenzel, and N. Wild, J. Geophys. Res. **87(A)**, 101 (1982).